Received: 23 July 2020 | Revised: 9 October 2020 | Accepted: 27 October 2020

DOI: 10.1002/jemt.23639

RESEARCH ARTICLE

MICROSCOPY RESEARCH & TECHNIQUE WILEY

An investigation of corrosive effects on zirconia with different crystal structures

Koray Soygun[1] | Ali Ozer[2] | Mehmet Cagatay Ulucan[3] | Giray Bolayir[4]

[1]Department of Prosthodontics, Faculty of Dentistry, Cukurova University, Adana, Turkey

[2]Department of Metallurgy and Material Engineering, Faculty of Engineering, Cumhuriyet University, Sivas, Turkey

[3]Kutahya Dental Health Hospital, Ministry of Health, Kutahya, Turkey

[4]Department of Prosthodontics, Faculty of Dentistry, Cumhuriyet University, Sivas, Turkey

Correspondence
Koray Soygun, Department of Prosthodontics, Faculty of Dentistry, Cukurova University, 01380 Adana, Turkey.
Email: koraysoygun@hotmail.com

Funding information
Sivas Cumhuriyet University Scientific Research Project, Grant/Award Number: DIS-182

Review Editor: Chuanbin Mao

Abstract

This study aimed to compare the time-related corrosive resistance in different corrosive solution environments after sintering of zirconia with different crystal structures. The zirconia samples were produced in pellet form as 12.7 × 3 mm. To determine the time-related corrosion resistance of the sintered samples in sodium carbonate (Na_2CO_3), sodium chloride (NaCl), and citric acid ($C_6H_8O_7$) solutions, the weights were measured at baseline then on the first and fifth days and the microhardness values were calculated. For the evaluation of surface appearance, images were obtained with a scanning electron microscope. The baseline microhardness values of the groups with 3 and 10 mol% yttria-stabilized zirconia samples were found to be 1,064 VHN and 1,079 VHN, respectively. The microhardness values of the groups with 3 mol% yttria-stabilized zirconia samples immersed in Na_2CO_3 1d (1,010 VHN) and 5d (1,060 VHN), and NaCl (1d (1,010 VHN) and 5d (1,055 VHN) were found to be affected more. The microhardness values of the sample group (1,064 VHN) with 10 mol% yttria doped zirconia which was left for 5 days in citric acid were found to be lower than the sample group (1,120 VHN) with 3 mol% yttria added. $C_6H_8O_7$ was seen to have a greater corrosive effect with increased yttria content and the microhardness value decreased. With longer duration of the samples of all the groups in $C_6H_8O_7$, NaCl, and Na_2CO_3 solutions, the surface characteristics of the samples were affected negatively. With prolonged immersion in the corrosive solutions, the resistance to the corrosion causing the changes in the surface topography of the samples was seen to decrease.

KEYWORDS

corrosion, microhardness, SEM, zirconium oxide

1 | INTRODUCTION

Zirconia has three main crystals, namely monoclinic, tetragonal, and cubic. At room temperature, zirconia is in the monoclinic phase, and at temperatures >1,170°C, it transforms to the tetragonal phase. This phase change causes a reduction in volume of approximately 5%. In the tetragonal phase, stable zirconia acquires a cubic crystal structure at temperatures higher than 2,370°C. However, during cooling of zirconia, the T-M phase change causes an increase in volume of approximately 3–4% (Gautam, Joyner, Gautam, Rao, & Vajtai, 2016). To stabilize zirconia in the tetragonal phase at room temperature, stabilizing oxides such as CaO, MgO, CeO_2, and Y_2O_3 are added in small amounts. Thus by preventing uncontrolled phase change, the material is obtained which is semistable at room temperature and this is known as partially stabilized zirconia (Gautam et al., 2016; Golieskardi, Satgunam, & Ragurajan, 2017; Kelly, 2004). Another factor to be effective in the phase change mechanism of the material is the amount of stabilizing oxide in the content. The addition of Y_2O_3 more than 8 mol

% to pure zirconia, prevents phase change and completely stabilizes the material to cubic in room temperature. The amount of Y_2O_3 added is important to provide the transformation hardening/toughnening mechanism which strengthens the material by preventing the progression of a crack occurring in a ceramic structure which is known as crack tip blunting and crack deflection (Gautam et al., 2016; Yilmaz, Aydin, & Gul, 2007).

Since the dental materials are exposed to various chemicals in the mouth, high resistance to corrosion is important (Corne, De March, Cleymand, & Geringer, 2019). Corrosion occurring with the electrical effect of a material is related to the electrode oxidation potential of that material, in other words, the minimum energy required for electrons to be broken from the material. However, higher the electrode oxidation potential of the material, the greater the resistance of the material to corrosion. Resistance to corrosion of a material is referred to as inertness, which is one of the most important properties of biomaterials. Corrosion creates serious problems of both deterioration of the prosthesis and the release of potentially toxic or allergic particles from the prosthesis (Lodi et al., 2018; Ozer, Soygun, & Bolayir, 2018; Winston Revie, 2000).

Fluctuations in pH, therefore in the chemistry of the solution, together with wear and mechanical loading make survival in the intraoral environment difficult. Liquid (aqueous) environments accelerate the progression of cracks in ceramic material (Guo et al., 2014; Guo et al., 2017). In addition to reduced mechanical resistance because of corrosion, the surface smoothness is impaired, plaque accumulates in productive areas, antagonist surface wear potentially increases, and aesthetics deteriorate. In addition, when the chemical stability of ceramics is impaired, there is an increased tendency for the release of inorganic ions (Guo et al., 2014; Moazzami et al., 2016).

The null hypothesis to be tested was that there was no difference between the corrosive resistance of zirconia ceramics with different polycrystalline structures.

2 | MATERIALS AND METHODS

2.1 | Preparation of the zirconia samples

With the addition of 3 and 10% Y_2O_3 to change the crystal structure by stabilizing zirconia, the obtaining of the tetragonal and/or cubic phase from the monoclinic phase of ZrO_2 was determined with XRD analysis (Figure 1).

To produce tetragonal and cubic zirconia, yttria was added at an amount of 3 mol% and 10 mol% to ytrria and zirconia powder 5–10 μm in size (Nanografi, Ankara, Turkey), and ground in a mill (MSETek, Kocaeli, Turkey), by mixing with 96% ethanol. As the milling medium, zirconia beads/powders were used in a ratio of 10:1 with 50 wt% of 5 mm and 50 wt% of 3 mm. Powder was eventually obtained by calcinating the milled and mixed powders at 1,000°C for 2 hr. The temperature of 1,000°C was reached by heating at 2°C/min and after a holding time of 2 hr, cooling was applied at 10°C/min.

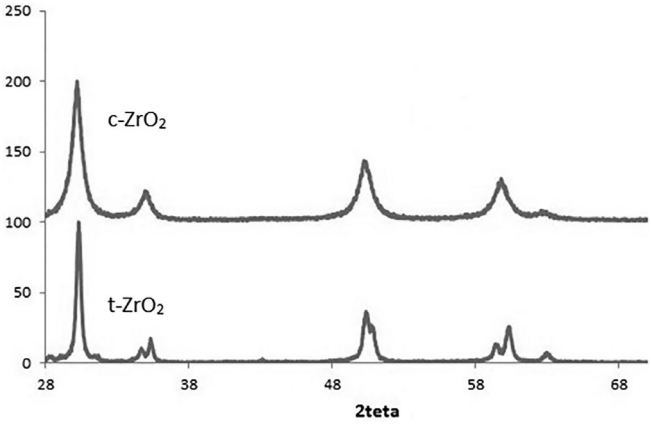

FIGURE 1 XRD patterns after calcination of the zirconia powders stabilized with yttria

The powders produced were compressed uniaxially, then compacted by cold isostatic compression. The zirconia samples were produced in the form of pellets with a 10-ton hydraulic press 12.7 mm in diameter and 3 mm thick.

2.2 | Preparation of the solutions

Sodium carbonate (Na_2CO_3), sodium chloride (NaCl), and citric acid ($C_6H_8O_7$) powders were purchased (Sigma-Aldrich, St. Louis, MO) to be used for the preparation of the solutions. Immersion solutions were prepared according to molecule weights to be in the form of 1 M. After the preparation of stock solutions of 1 L each, daily solution refreshing procedures were applied. A 1-day and 5-day static immersion system was applied for all the samples. The solutions were kept in 100 ml closed beakers at 25 ± 2°C. Clear solutions were obtained to be stable in a still environment. By replenishing the solutions, stock solutions were kept fresh without any potentially undissolved residue. To be able to provide the mechanical stability and/or chemical reaction stability on the surfaces of the zirconia samples and to avoid nucleation or accumulation in the beakers, the samples were suspended vertically.

The solutions were used to simulate the oral environment in soda or mineral water, Na_2CO_3 is in the dissolved state, and precipitation produces Na_2CO_3 crystals. Sometimes the precipitation may occur as sodium bi-carbonate in the presence of OH. NaCl was used in this study to represent salty food/drink consumption such as turnips and, lentil soup. $C_6H_8O_7$ was used to represent citrus fruits, especially lemons, oranges, and grapefruit, and precipitates as thick film of $C_6H_8O_7$ on the teeth.

2.3 | Weight loss measurement test

In the examination of the corrosive properties of the samples of all groups in the study, the weight of the samples at baseline was

measured using precision scales (Shimadzu AX120, Shimadzu Co., Ltd., Kyota, Japan) with 0.001 g. sensitivity. After exposure to the solutions, prepared at different pHs for 1 and 5 days, the samples were weighed again using the same scales.

2.4 | Microhardness test

Surface microhardness measurements of the samples of each sample group were made using a microhardness device (Buehler MMT-3 digital microhardness tester, Lake Bluff, IL). The surface microhardness values of the samples measured by applying a 500 g load applied for 30 s at room temperature of 23 ± 1°C were recorded as Vickers hardness units. For each sample, five measurements were taken not closer than 1 mm to each other in the central region or not closer than 1 mm to the edges. The mean of these measurements was accepted as a single value for each sample.

2.5 | Scanning electron microscope and element analysis

To evaluate the images of the surface topography, one sample was chosen randomly from the groups and assumed as identical by sintering in different crystal structures for scanning electron microscope (SEM) analysis. First, to decrease the scattering and charging of electron beam, the samples were coated with approximately 5 nm gold for 120 s (QUORUM ES150R, UK). Surface topography was visualized with SEM (TESCAN Mira3 XMU, Brno, Czechia). At the same time, energy dispersive spectroscopy (EDS) element analysis was applied (Oxford Inst., INCA x-act, UK) to determine. The amount of elements in the region struck by the electron beam. As these were determined in parallel, all elements were defined at the same time.

3 | RESULTS AND DISCUSSION

This study was designed to evaluate the corrosive resistance of zirconia ceramics with different polycrystalline structures. The null hypothesis to be tested was that there was no difference between the corrosive resistance of zirconia ceramics with different polycrystalline structures. The null hypothesis was supported by the findings of the study.

To produce tetragonal and cubic stabilized zirconia, yttrium oxide was selected, the addition of which at small amounts can provide transformation of zirconia in the tetragonal and cubic system when added as 3 mol% Y_2O_3 and 10 mol% Y_2O_3, respectively. The XRD analysis patterns following the calcination of tetragonal and cubic zirconia are shown in Figure 1.

As seen in Figure 1, more than 95% partially stabilized tetragonal zirconia was produced with a small amount of monoclinic zirconia seen at 2-theta degrees of around 29° and 31° 2-theta. The formation of tetragonal peaks was determined with peak separations seen at 35, 50, and 60° 2-theta due to c-axis formation in the tetragonal structure. In contrast, the cubic zirconia was obtained fully stabilized with the addition of 10 mol% Y_2O_3 with a fine primary crystallite size of 33 ± 7 nm.

As can be seen in Figure 2, the rate of temperature rise was kept very low to allow sufficient transformation and a high sintering density to be obtained. A rapid cooling rate was chosen to avoid cubic/tetragonal to monoclinic transformation around 1,000°C and it was aimed to avoid cracks or deformations in the samples by structural expansion. Thus, an increase in the density of the structure was obtained and there was no excessive (abnormal) grain growth.

Keeping the sintering cycle at 1,550°C in the oxide furnace, sintering of the samples reached up to approximately 98% of relative density, but because of the long periods in the heating and cooling regime, some large and abnormal grains were seen in the structure (Figure 3). Pores at the triangles of grains were seen to interfere with the grain growth and the sudden growth of grains makes the pores larger and the grains coarser. This leads to a reduction in relative density from 99.5 to 98%, known as dedensification. A reduction in corrosion resistance can be expected because of penetration of the solution to the pores and chemical affinity of abnormal grains to the corrosive media.

The EDS method, which can be defined as a chemical microanalysis technique, can be applied using an SEM. In the EDS method, the element content of the examined surface can be determined by analyzing X-rays reflected from the sample surface on which the electron bundle is directed (Newbury & Ritchie, 2013). When the electron is directed to the sample under the SEM, electrons that are scattered from the atoms formed on the sample surface, and electrons coming from higher energy shells fill these gaps and X-rays are released to balance the energy difference between these two electrons. The energy level of each X-ray varies according to the specific element over which it is released. The amounts and energies of these beams are measured with an EDS X-ray detector, and thus, qualitative and semiquantitative determinations of elements in the sample content can be obtained. In addition, by creating an element map of the examined surface, the rates and distribution of the elements in the surface

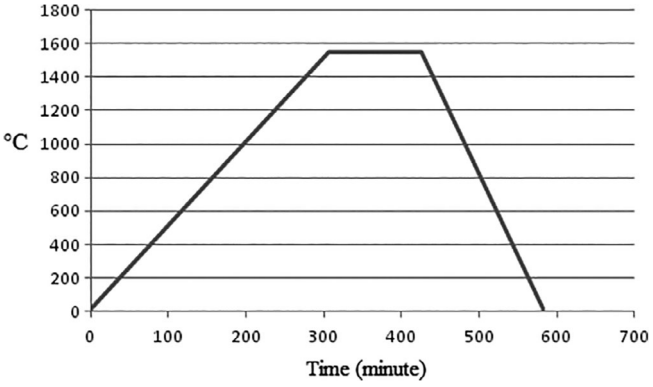

FIGURE 2 Temperature-heating time graph of the sintering regime

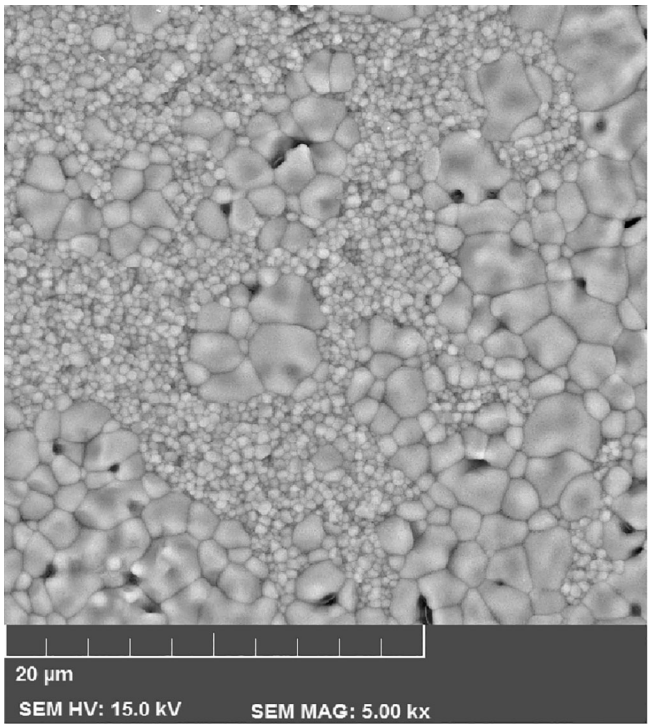

FIGURE 3 Scanning electron microscope (SEM) image of zirconia pellet sintered at 1,550°C

can be visually determined (Newbury & Ritchie, 2013; Soygun, Soygun, & Dogan, 2020).

Surface photographs of tetragonal zirconia (3YSZ) samples that have undergone corrosion in different environments for 1 and 5 days can be seen in Figure 4. With immersion for 1 day, the grain boundaries on the surface of tetragonal zirconia were observed to have dissolved and although the particles of precipitates were thin, they had started to accumulate around other large grains. These precipitates are known as nuclei regions of the 1d immersion and can be thought to indicate an increased possibility of larger crystals accumulating on similar regions later. In the element analysis with EDX, there was seen to be approximately 13 wt% carbon (4a) and this was thought to originate from the CH of $C_6H_8O_7$. In Figure 4b), approximately 10 wt% carbon can be seen, which may and also come from carbonate. In Figure 4c, the presence of Na in (b) and (c) comes from cations of NaCl and Na_2CO_3, and the presence of Cl in (c) from anion.

In the deposits of the 5 days immersions seen in Figure 4(d-e-f), it can be seen that the crystals formed have grown in size and there are positive weight difference of the accumulations. The majority of the structure in the 5 days immersion in $C_6H_8O_7$ is covered with acid remnants and the presence of hydrocarbon residues originating from CH of acid remnants formed as a thick film layer can be seen (d). As a weight difference of 37% was found in the carbon elemental count, this indicates the presence of CH coating the surface. The coating is so effective that the structures of the surface grains are barely seen. The small nuclei shown in (b) can be seen to have grown in (e) and have attached to the surface by partially embedding and there can be seen to be a tendency to progress inwards. In the element analysis, Na-carbonate precipitation is seen by combining the increased C and O with increased Na. Similarly in (f) with increased Na-Cl filling the gaps between the grains of the structure, salt crystals have grown and formed around salt nuclei.

It can be seen that the structure has formed with $C_6H_8O_7$ as a film coating and carbonated salt in the form of proliferation of the nuclei and the gathering of chloride salt from the solution around the nucleus.

One of the parameters determining the surface behavior of ceramic materials which are located in a continuously wet environment in the mouth, is the "zeta potential." Zeta potential (electric potential on the surface) is the measurement of the attraction and repulsion value between particles. When the zeta potential of glass materials approaches zero, the hardness values increase, and when surface energy increases positively, they become softer. As the oral cavity is a wet environment, positive loads forming on the glass or ceramic surface, reduce surface hardness with the passing of sodium ions to the liquid environment (Chatzistavrou et al., 2014; Figueiredo-Pina et al., 2016). Therefore, ceramics display different behaviors depending on the interactions of the components forming the microstructures with the surroundings.

Surface photographs of cubic zirconia samples (10YSZ) that have undergone corrosion in different environments for 1 and 5 days can be seen in Figure 5. With immersion for 1 day, the dissolving of the grain boundaries on the surface of cubic zirconia is seen together with the start of aggregation of precipitate particles around the grains. These deposits with 1 day immersion are known as nucleus regions and an increased possibility of larger crystals accumulating here is also expected later. Small scattered nuclei can be seen in the structure in (b) and very small deposits of chlorides can be seen on Figure 5c. As seen on Figure 5a–c, there was a huge difference in nucleation from 1 to 5 days of immersion and with increasing days, the accumulation of $C_6H_8O_7$ and other salts was attributed to CH, carbonate and chloride. In Figure 5b, precipitations can be seen, originating from carbonate.

In the deposits of the 5 days immersions, it can be seen that the crystals formed have grown in size and there are positive weight difference of the deposits. Almost the whole surface structure in the 5 days immersion in $C_6H_8O_7$ is covered with a thick layer of acid carbonaceous remnant that indicates the presence of CH (Figure 5d). The coating is so effective that the structures of the grains on the surface cannot be seen. The small nuclei shown in (b) can be seen to have grown in (e) and have attached partially penetrating into the surface. In the element analysis, Na-carbonate precipitation is seen by increased Na, C, and O. Similarly in (f) with increased Na-Cl and by filling the gaps between the grains of the structure, salt crystals have grown and formed around salt nuclei.

The weight loss values of the sintered and densified samples at the end of 1 and 5 days immersion are shown in Table 1. The increased carbonate deposits on the fifth day with small deposits on the first day led to loss. The weight loss concept is based on the dissolution of materials into aqueous solution but not accumulation and embedding onto the surface. Therefore, the increase in weight should

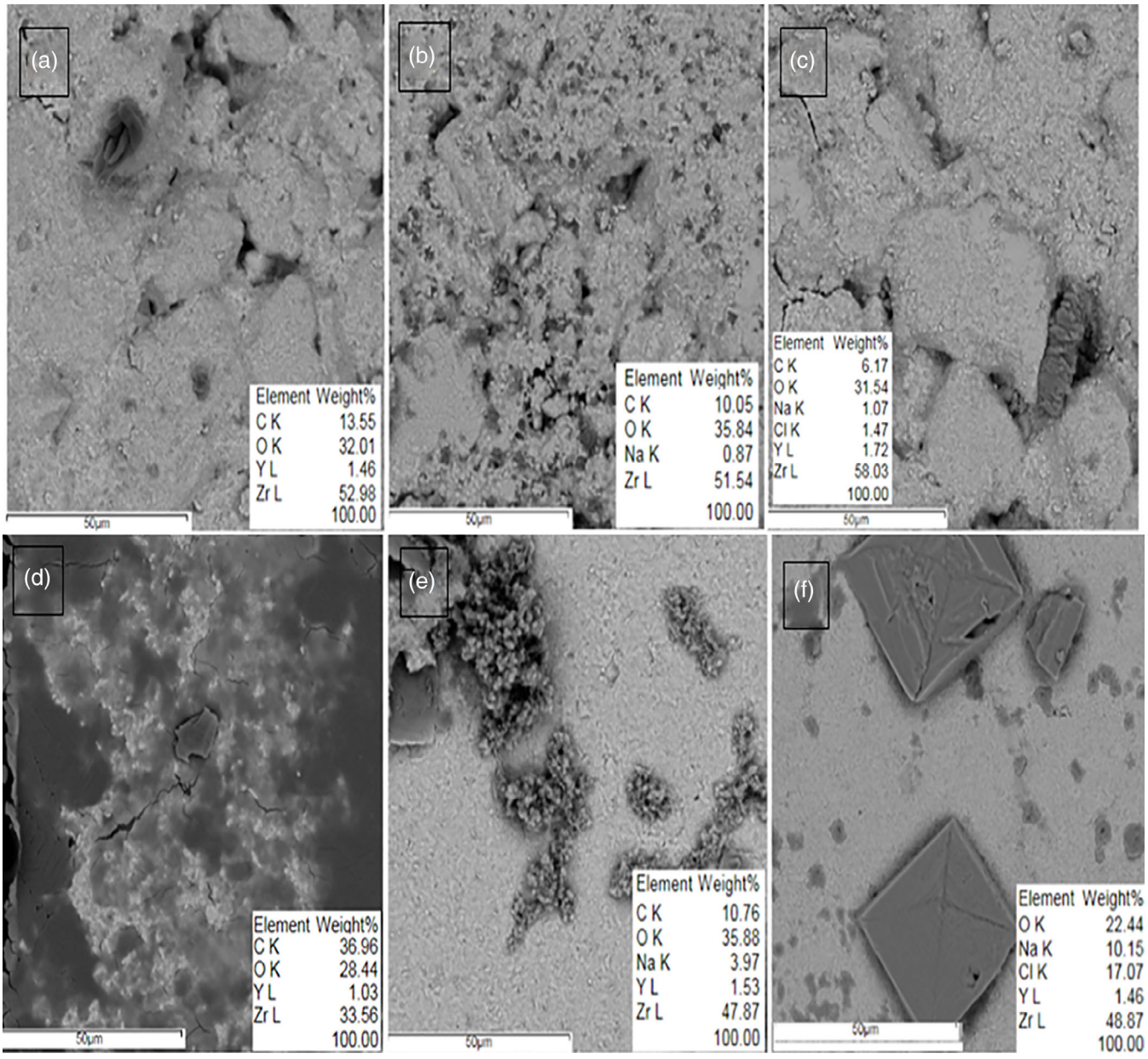

FIGURE 4 Scanning electron microscope (SEM)–BSE surface images and element count from EDX analysis of 3YSZ sintered samples at 1 day in (a) $C_6H_8O_7$, (b) Na_2CO_3, and (c) NaCl, and at 5 days in (d) $C_6H_8O_7$, (e) Na_2CO_3, and (f) NaCl

be understood as accumulation on the surface while the main material has dissolved into the solution but not to as great an extent as the accumulation which has resulted in the weight increase. In contrast, the deposits of chloride salt on the surface with increased immersion time showed an increase in weight. This result can be interpreted as the salts accumulating in the surface pores or roughness increases inwards, and that they are attached to the zirconia surface by forming a nuclei root. In addition, although it is necessary to remove all kinds of deposit causing a weight increase from the surface with hot water or continuous washing, salt and carbonate deposits may have again settled on the surface during rinses from the surface and then dried on the surface. Although there are similar conditions in $C_6H_8O_7$ immersion, it is difficult to remove the film layer from the surface. The increased weight loss at 5 days in particular is shown in 3YSZ, and this was thought to be due to the $Zr(OH)_4$ ionization because of the presence of both CH and OH, and removal from the pores and undergoing corrosion.

The difference in hardness resulted from the solutions and the immersion times are shown in Figure 6 and Table 2. On the first day, nucleus deposits of the carbonate and chloride solutions could not be measured but were thought to be almost close to pure materials. With increasing durations, an increase was seen in hardness with deposits entering between pores and grain boundaries especially for NaCl and Na_2CO_3 deposition on the surface due to salt accumulation between grains. On the yellow and orange graphs, the immersion time of 10YSZ is shown. As the deposit size in carbonate solution had

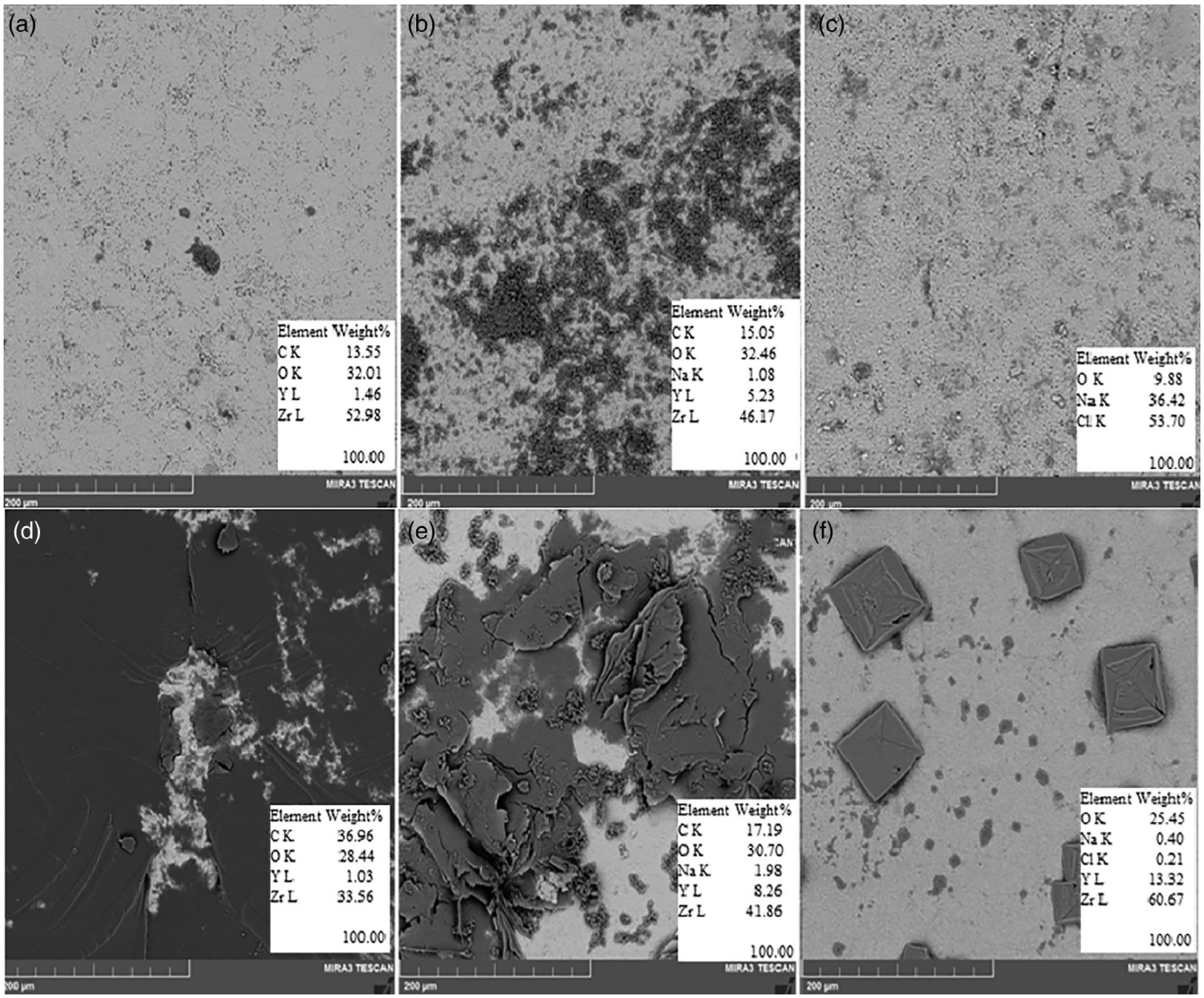

FIGURE 5 Scanning electron microscope (SEM)–BSE surface images and element count from EDX analysis of 10YSZ sintered samples at 1 day in (a) $C_6H_8O_7$, (b) Na_2CO_3′e, and (c) NaCl, and at 5 days in (d) $C_6H_8O_7$, (e) Na_2CO_3′e, and (f) NaCl

TABLE 1 Weight loss percentages (g) of the sample groups in the different immersion solutions

	3YSZ		10YSZ	
	1 day	5 days	1 day	5 days
Na_2CO_3	−0.77922	1.01010	0.72057	0.90012
NaCl	0.04357	−0.49801	−0.08196	−0.28513
$C_6H_8O_7$	−0.34483	1.42857	−0.28420	−0.08928

Abbreviations: $C_6H_8O_7$, citric acid; Na_2CO_3, sodium carbonate; NaCl, sodium chloride.

increased, although no decrease was seen to have formed from the dissolved zirconia, there was a drastic deformation with hardness of the films on the first and fifth days together with increasing $C_6H_8O_7$ film coverage, and there was a reduction in hardness with the increasing thickness and the time of immersion. It can therefore be concluded that the more elastic organic structure of $C_6H_8O_7$ leads to deeper penetration of indentations, resulting in lower Vickers hardness values.

4 | CONCLUSION

In this in vitro study of zirconia with different crystal structures, the samples sintered using the traditional sintering method followed by immersion for 1 and 5 days in $C_6H_8O_7$, NaCl and sodium bicarbonate solutions, and the weight loss values, microhardness values, and SEM results of the sample groups are summarized as follows:

- The zirconia powders were produced in tetragonal and cubic form according to XRD as a stabilized form and pellets were pressed and

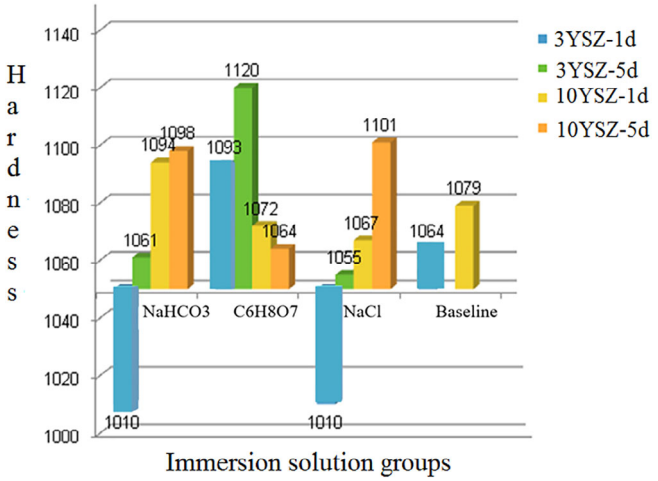

FIGURE 6 Changes in microhardness of the samples according to the immersion times in the solutions [Color figure can be viewed at wileyonlinelibrary.com]

TABLE 2 Vickers microhardness values of the sample groups according to the duration of immersion in the solutions (VHN)

	3YSZ		10YSZ	
	1 day	5 days	1 day	5 days
Na_2CO3	1,010	1,061	1,094	1,098
$C_6H_8O_7$	1,093	1,120	1,072	1,064
NaCl	1,010	1,055	1,067	1,101
Baseline	1,064		1,079	

Abbreviations: $C_6H_8O_7$, citric acid; Na_2CO_3, sodium carbonate; NaCl, sodium chloride.

sintered to observe the effect of corrosive mediums on the surfaces.

- The highest microhardness values were obtained from the cubic phase zirconia samples since cubic zirconia has the highest hardness of the crystal polymorphs of zirconia in pure form.
- The sample groups with different crystal structures obtained with the traditional sintering method were affected by the corrosive solutions used in the study.
- As the immersion times within the corrosive solutions increased, the surface properties of the samples were drastically affected and the accumulated surface layer of $C_6H_8O_7$ resulted in an extensive decrease in zirconia hardness. In the zirconia sample with accumulated carbonate and chloride, hardness increased due to deposition of those salts among the grains to reduce the pores.
- The SEM analysis showed that zirconia samples were sintered and densified up to 98% of relative density. The surfaces were examined with SEM after immersion in different solutions for different time periods and the solution precipitates were seen to have grown on all the surfaces by either penetrating into the structure or coating as a film.

ACKNOWLEDGMENTS

The authors do not have any financial interest in the companies whose materials are included in this article. The study was partly supported number of DIS-182 by Sivas Cumhuriyet University Scientific Research Project. A part of this study was conducted in SEM Facility of Sivas CU Research & Development Center (CUTAM).

CONFLICT OF INTEREST

The authors declare no conflict of interest.

ORCID

Koray Soygun https://orcid.org/0000-0002-0145-3947

REFERENCES

Chatzistavrou, X., Fenno, J. C., Faulk, D., Badylak, S., Kasuga, T., Boccaccini, A. R., & Papagerakis, P. (2014). Fabrication and characterization of bioactive and antibacterial composites for dental applications. *Acta Biomaterialia*, *10*(8), 3723–3732.

Corne, P., de March, P., Cleymand, F., & Geringer, J. (2019). Fretting-corrosion behavior on dental implant connection in human saliva. *Journal of the Mechanical Behavior of Biomedical Materials*, *94*, 86–92.

Figueiredo-Pina, C. G., Patas, N., Canhoto, J., Cláudio, R., Olhero, S. M., Serro, A. P., … Guedes, M. (2016). Tribological behaviour of unveneered and veneered lithium disilicate dental material. *Journal of the Mechanical Behavior of Biomedical Materials*, *53*, 226–238.

Gautam, C., Joyner, J., Gautam, A., Rao, J., & Vajtai, R. (2016). Zirconia based dental ceramics: Structure, mechanical properties, biocompatibility and applications. *Dalton Transactions*, *45*(48), 19194–19215.

Golieskardi, M., Satgunam, M., & Ragurajan, D. (2017). Effect of holding time on the mechanical properties and microstructural evaluation of 3Y-TZP ceramics. *Journal of the Australian Ceramic Society*, *53*(2), 1001–1006.

Guo, J., Li, D., Wang, H., Yang, Y., Wang, L., Guan, D., … Zhang, S. (2017). Effect of contact stress on the cycle-dependent wear behavior of ceramic restoration. *Journal of the Mechanical Behavior of Biomedical Materials*, *68*, 16–25.

Guo, J., Tian, B., Wei, R., Wang, W., Zhang, H., Wu, X., … Zhang, S. (2014). Investigation of the time-dependent wear behavior of veneering ceramic in porcelain fused to metal crowns during chewing simulations. *Journal of the Mechanical Behavior of Biomedical Materials*, *40*, 23–32.

Kelly, J. R. (2004). Dental ceramics: Current thinking and trends. *Dental Clinics of North America*, *48*(2), 513–530.

Lodi, E., Weber, K. R., Benetti, P., Corazza, P. H., Della Bona, Á., & Borba, M. (2018). How oral environment simulation affects ceramic failure behavior. *The Journal of Prosthetic Dentistry*, *119*(5), 812–818.

Moazzami, S. M., Zadeh, S., Kianoush, K., Sarmad, M., Barani Karbaski, F., Amiri Daluyi, R., & Kazemi, R. B. (2016). Chemical stability of bioglass in simulated oral environment. *Journal of Dental Biomaterials*, *3*(3), 261–268.

Newbury, D. E., & Ritchie, N. W. (2013). Is scanning electron microscopy/energy dispersive X-ray spectrometry (SEM/EDS) quantitative? *Scanning*, *35*(3), 141–168.

Ozer, A., Soygun, K., & Bolayir, G. (2018). The surface and phase analysis studies on dental bioceramics subjected to different mouthrinse solutions. *Journal of the Australian Ceramic Society*, *54*(3), 475–481.

Soygun, K., Soygun, A., & Dogan, M. C. (2020). The effect of gastric acid on chitosan modified glass ionomer cement: SEM-EDS. *Microscopy Research and Technique*, *83*(1), 3–9.

Winston Revie, R. (2000). *Corrosion of refractories and ceramics, Uhllig's corrosion handbook*. Canada: John Wiley & Sons.

Yilmaz, H., Aydin, C., & Gul, B. E. (2007). Flexural strength and fracture toughness of dental core ceramics. *The Journal of Prosthetic Dentistry*, *98*(2), 120–128.

How to cite this article: Soygun K, Ozer A, Ulucan MC, Bolayir G. An investigation of corrosive effects on zirconia with different crystal structures. *Microsc Res Tech*. 2020;1–8. https://doi.org/10.1002/jemt.23639